Colorimetric assay for ultrasensitive detection of phosphate in water bodies based on metal-organic framework nanospheres possessing catalytic activity

Jiayan Wang,[ab] Wenying Li,[a]* Yue-Qing Zheng[a]*

[a]Chemistry Institute for Synthesis and Green Application, School of Materials Science and Chemical Engineering, Ningbo University, Ningbo 315211, Zhejiang, PR China.

[b]Medical School, Ningbo University, Ningbo 315211, Zhejiang, PR China.

*Corresponding author:

Email: liwenying@nbu.edu.cn

Fax: +86-574-8760074

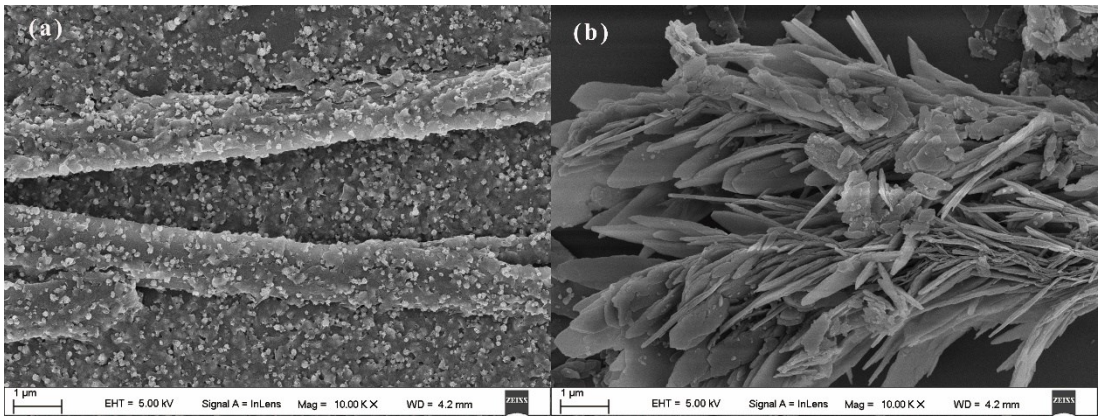

Figure S1. SEM image of other two Cu-MOFs (a) The ligand is 2-Aminoterephthalic acid. (b) The ligand is nitroterephthalic acid.

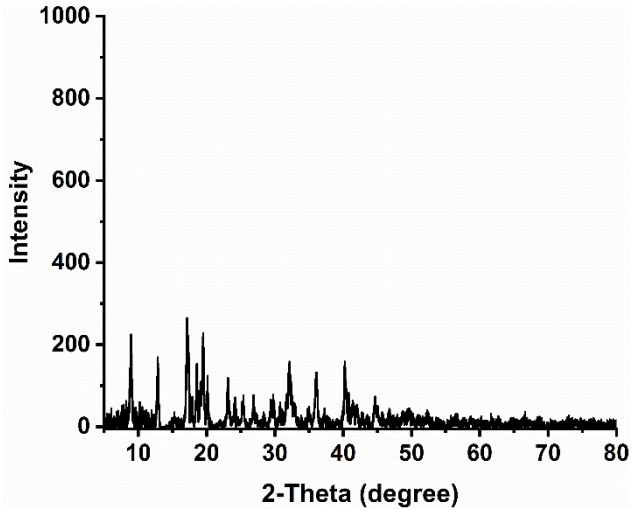

Figure S2 Powder X-ray pattern of Cu-MOF(3).

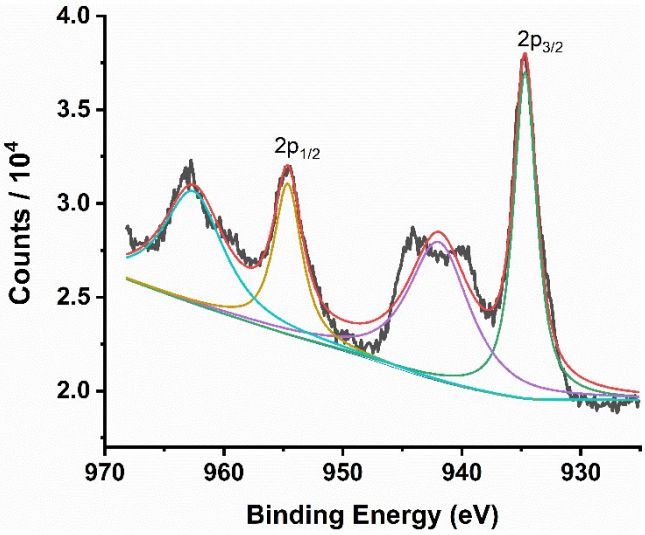

Figure S3. High resolution XPS pattern of Cu elements in Cu-MOF(3).

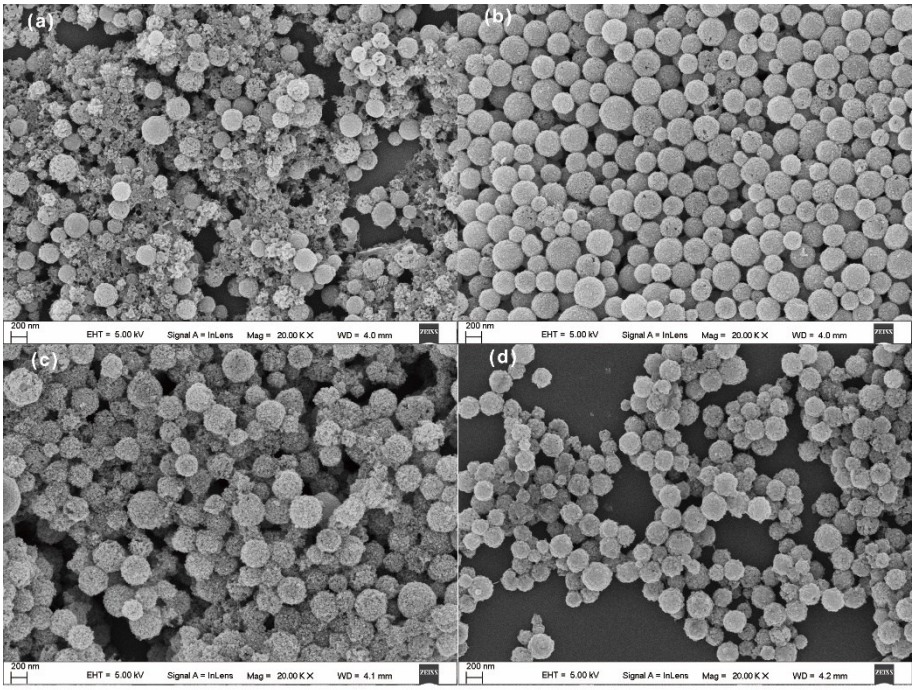

Figure S4. SEM images of Cu-MOF nanospheres obtained after different reaction time (a) 4 h, (b) 8 h, (c) 12 h, (d) 16 h.

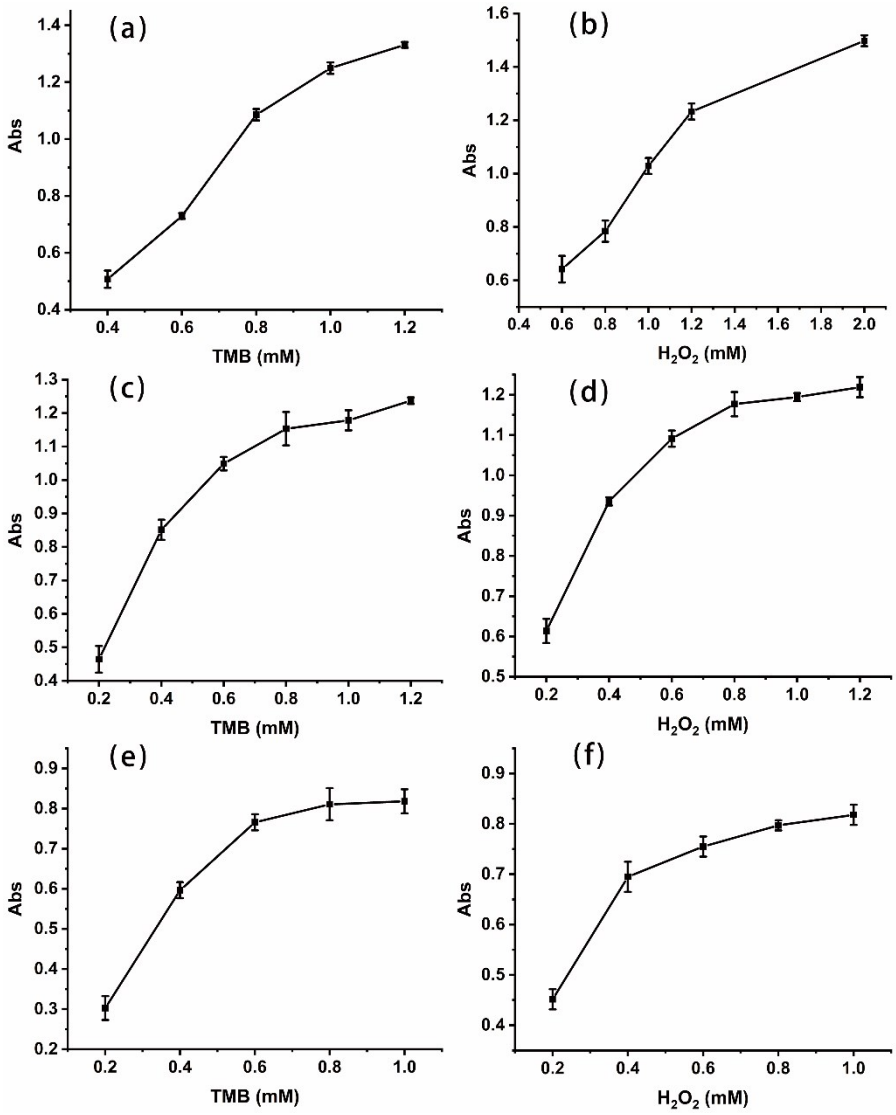

Figure S5. Steady state kinetic assays. Changes of absorbance at 652 nm of TMB-H_2O_2 system in the presence of (a) Cu-MOF(1), (c) Cu-MOF(2) or (e) Cu-MOF(3), and the H_2O_2 concentration was fixed at 1 mM. Changes of absorbance at 652 nm of TMB-H_2O_2 system in the presence of (b) Cu-MOF(1), (d) Cu-MOF(2) or (f) Cu-MOF(3), and the TMB concentration was fixed at 0.8 mM.

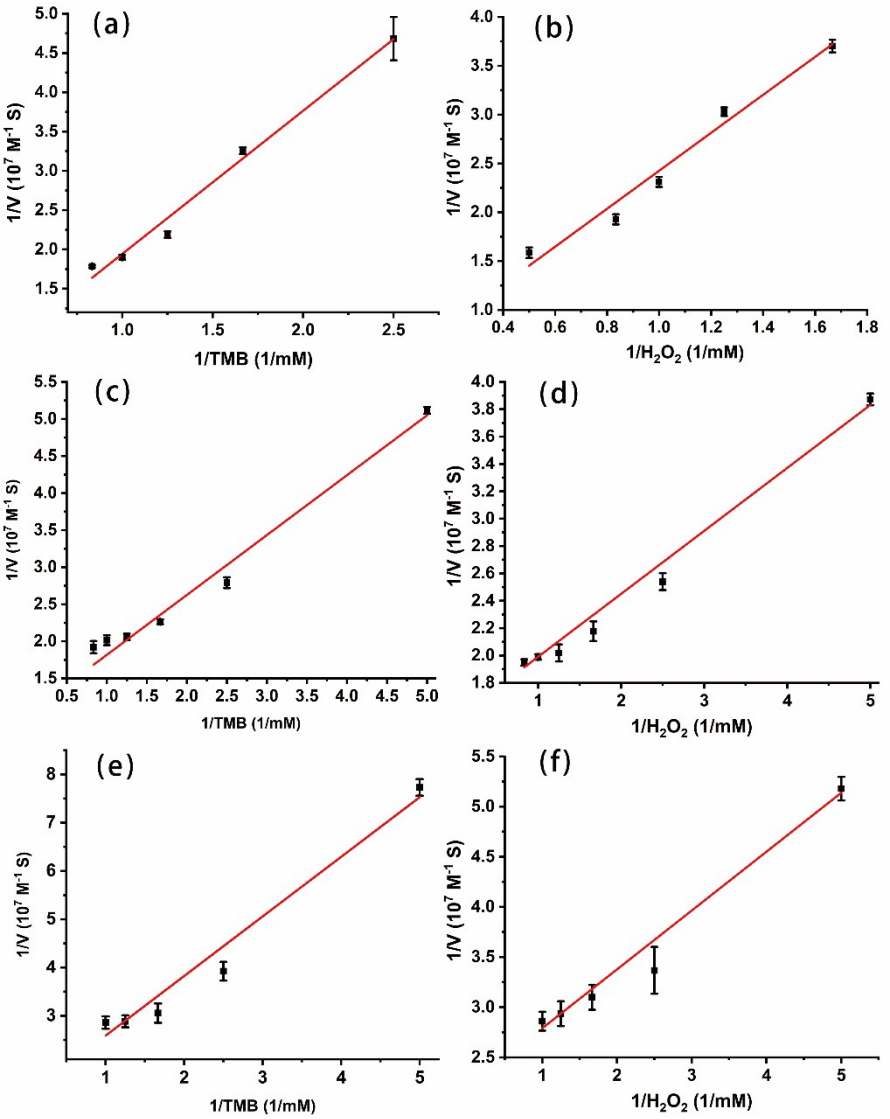

Figure S6. Steady-state kinetic analyses using the Lineweaver-Burk model for Cu-MOF(1) ((a) and (b)), Cu-MOF(2) ((c) and (d), Cu-MOF(e) ((a) and (f))).

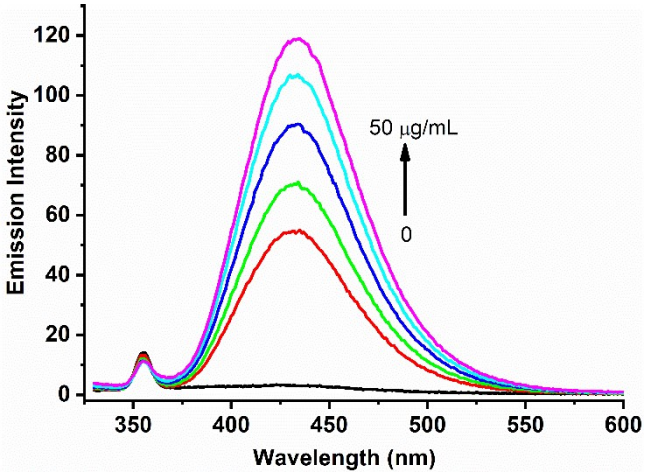

Figure S7. Fluorescence of terephthalic acid after reacted with OH• radicals generated by Cu-MOF nanospheres with different concentrations. Bottom to up: the concentrations of Cu-MOF nanospheres was 0, 10, 20, 30, 40, 50 μg/mL.

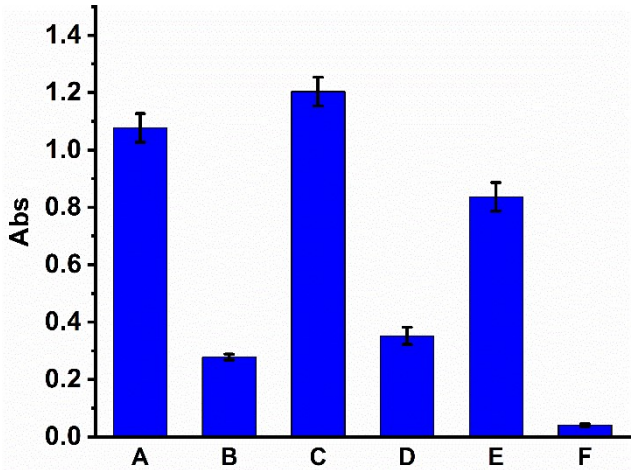

Figure S8. Absorbance at 652 nm of different reaction system. A: Cu-MOF(1), B: Cu-MOF(1)+phosphate, C: Cu-MOF(2), D: Cu-MOF(2)+phosphate, E: Cu-MOF(3), B: Cu-MOF(3)+phosphate.

Figure S9. Digital images of the Cu-MOF/TMB-H_2O_2 system with different concentrations of phosphate: from left to right are 0, 0.05, 0.125, 0.25, 0.5, 1, 3 and 5 μM.

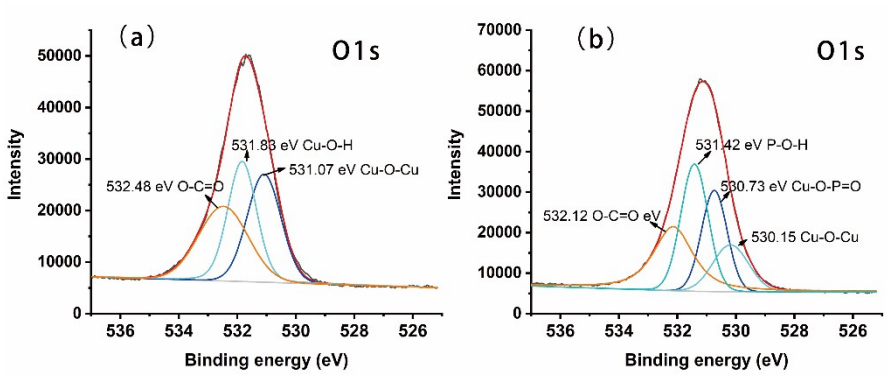

Figure S10 High resolution XPS pattern of O1s in Cu-MOF(3) (a) before and (b) after reaction with phosphate.

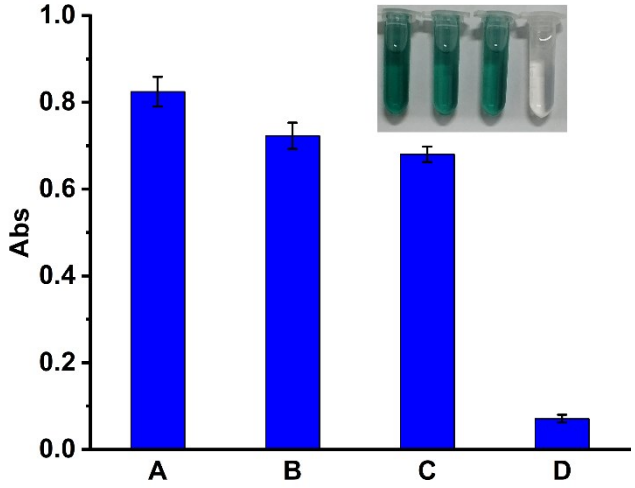

Figure S11 Absorbance at 652 nm of TMB+H_2O_2 systems in the presence of Cu-MOF(3) (A), Cu-MOF(3)+arsenate (B), Cu-MOF(3)+arsenite (C) or Cu-MOF(3)+arsenate. Inset was the photo of corresponding systems (from left to right).The concentrations of arsenate, arsenite and phosphate are all 20 μM.

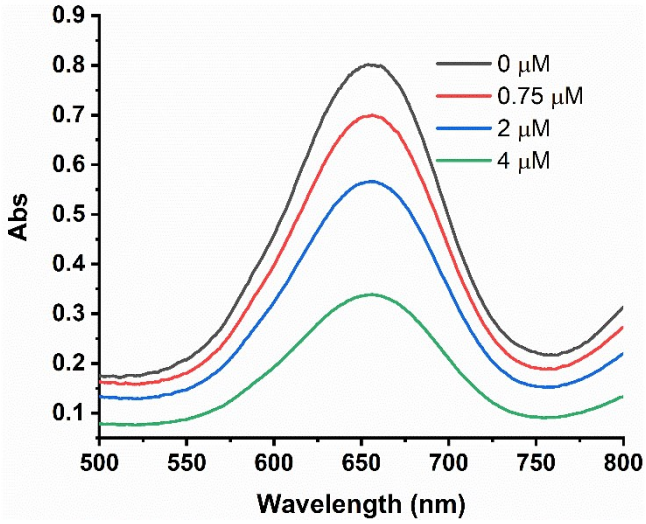

Figure S12. Detection of phosphate in river water samples. 0.75, 2 and 4 μM phosphate were spiked to the assay system, respectively.

Table S1 Comparison of Cu-MOF nanospheres with HRP and Fe_3O_4.

	Substrate	*Km* (mM)	*Vmax* (M s^{-1})
HRP	TMB	0.434	3.44×10^{-8}
HRP	H_2O_2	3.7	9.78×10^{-8}
Fe_3O_4	TMB	0.098	3.44×10^{-8}
Fe_3O_4	H_2O_2	154	9.78×10^{-8}
Cu-MOF(1)	TMB	15.04	8.25×10^{-7}
Cu-MOF(1)	H_2O_2	4.04	2.07×10^{-7}
Cu-MOF(2)	TMB	0.80	1.00×10^{-7}
Cu-MOF(2)	H_2O_2	0.30	6.53×10^{-8}
Cu-MOF(3)	TMB	1.05	8.31×10^{-8}
Cu-MOF(3)	H_2O_2	0.273	4.65×10^{-8}

Table S2 Comparison of phosphate detection methods.

Detection technique	Sensor description	Range (μM)	LOD (μM)	Interferences	Reference
Electrochemical	Paper-based screen-printed electrode	~300	4		[1]
Fluorescence	lanthanide MOF	0.1~15	0.052		[2]
Fluorescence	morin-hydrotalcite complex	100-10000	32	CO_3^{2-}	[3]
Fluorescence	Zr-based MOF/ rhodamine B	80 to 400	2		[4]
Colorimetric	Fe_3O_4 nanocubes/Zr^{4+}	0.066-33.3	0.0498		[5]
Colorimetric	silver nanoplates/Eu^{3+}	6-183	2		[6]
Fluorescence	Disposable wax-printed paper strip	0.001-0.064	0.001	NaCl, F^-, $MgCl_2$, NO_3, and KCl	[7]
Fluorescence	CIP-Eu^{3+} /SDBS	0.02-4	0.004		[8]
Fluorescence	Zr based metal-organic frameworks	5-150	1.25		[9]
Fluorescence	lanthanide functionalized coordination polymer	5-150	0.88		[10]
Fluorescence	phenanthro[9,10-d]imidazole-coumarin	Not mentioned	0.14		[11]
Colorimetric	Cu-MOF/TMB-H_2O_2 system	0.05-5	0.02		This method

References

1. S. Cinti, D. Talarico, G. Palleschi, D. Moscone and F. Arduini, *Anal. Chim. Acta*, 2016, **919**, 78-84.
2. Y. Cheng, H. Zhang, B. Yang, J. Wu, Y. Wang, B. Ding, J. Huo and Y. Li, *Dalton Trans.*, 2018, **47**, 12273-12283.
3. H. D. Duong and R. Jong Il, *Sens. Actuators B Chem.*, 2018, **274**, 66-77.
4. N. Gao, J. Huang, L. Wang, J. Feng, P. Huang and F. Wu, *Appl. Surf. Sci.*, 2018, **459**, 686-692.
5. X. Li, B. X. Liu, K. Ye, L. Ni, X. C. Xu, F. X. Qiu, J. M. Pan and X. H. Niu, *Sens. Actuat. B Chem.*, 2019, **297**, 126822.
6. C. Pinyorospathum, P. Rattanarat, S. Chaiyo, W. Siangproh and O. Chailapakul, *Sens. Actuat. B Chem.*, 2019, **290**, 226-232.
7. M. Sarwar, J. Leichner, G. M. Naja and C. Z. Li, *Microsyst. Nanoeng.*, 2019, **5**, 56.
8. H. Wu and C. Tong, *ACS Sens.*, 2018, **3**, 1539-1545.
9. J. Yang, Y. Dai, X. Y. Zhu, Z. Wang, Y. S. Li, Q. X. Zhuang, J. L. Shi and J. L. Gu, *J. Mater. Chem. A*, 2015, **3**, 7445-7452.
10. Y. Zhang, S. Sheng, S. Mao, X. Wu, Z. Li, W. Tao and I. R. Jenkinson, *Water Res.*, 2019, **163**, 114883.
11. B. Zhao, T. Liu, Y. Fang, L. Y. Wang, W. Kan, Q. G. Deng and B. Song, *Sens. Actuat. B Chem.*, 2017, **246**, 370-379.